Energy & Buildings 235 (2021) 110726

Contents lists available at ScienceDirect

Energy & Buildings

journal homepage: www.elsevier.com/locate/enb

Experimental investigation of sustainable and energy efficient management of a geothermal field as a heat source and heat sink for a large office building

Kristian Duus *, Gerhard Schmitz

Hamburg University of Technology, Institute of Engineering Thermodynamics, Denickestrasse 17, 21073 Hamburg, Germany

ARTICLE INFO

Article history:
Received 16 October 2019
Revised 3 September 2020
Accepted 2 January 2021
Available online 6 January 2021

Keywords:
Large office building
Monitoring
Energy efficiency
Sustainability
Thermal concrete core activation
Shallow geothermal energy
Heat pump
Distributed Temperature Sensing
Model predictive control
Experimental

ABSTRACT

The new construction of a large office building in Hamburg, which is the subject of this investigation, has been closely monitored over a period of about 5 years. In addition to evaluating and optimising the energy demands and user comfort, the focus was on the management of the energy from an exceptionally large geothermal field which is used for heating and cooling the building. The possibilities for sustainable, energy efficient use of the geothermal field were investigated. The basis for the evaluations is a fibre optic Distributed Temperature Sensing (DTS) system, by means of which temperature profiles in the ground as well as in the concrete of the energy piles are recorded on an ongoing basis. With regard to the impact of geothermal energy use on the environment, the surrounding soil may be considered as undisturbed to date, based on the corresponding ground temperature measurements. The ground temperature measurements within the geothermal field show that by carrying out manual operating adjustments, ultimately the original soil temperature level could be achieved once again, after the three operating years under examination. A long-term, sustainable and therefore energy efficient use of the geothermal field is thus fundamentally possible in the present case.
© 2021 The Authors. Published by Elsevier B.V. This is an open access article under the CC BY license (http://creativecommons.org/licenses/by/4.0/).

1. Introduction

In terms of reducing greenhouse gas emissions, the focus is inter alia on the building sector. In the Federal Republic of Germany, more than one third of the total final-energy consumption is associated with buildings [1]. Ambitious targets for reducing greenhouse gas emissions have therefore been defined at both national and state level, which will be enforced by means of corresponding specified standards. Accordingly, the Hamburg Climate Plan [2], developed by the Senate in line with the national guidelines, stipulates a gradual reduction of CO_2 emissions by at least 40% by 2020, 50% by 2030 and 80% by 2050 compared to 1990. The targets for the building sector can only be achieved by improving the energy efficiency of buildings, in combination with an energy supply for buildings which is increasingly based on renewable energy sources. In accordance with the Integrated National Energy and Climate Plan [1] and the Hamburg Climate Plan [2], the long-term goal for 2050 can be achieved through different variations of the combination of improved energy efficiency and increasing use of renewable energy. The realistic range of options extends from a combination of 67% renewable energies in the energy supply and a 40% reduction in the energy consumption of buildings, right through to a combination of 50% renewable energies and a 60% reduction in the energy consumption of buildings. The new construction of a large office building in Hamburg, which is the subject of this investigation, is a showpiece project featuring high energy efficiency as well as an energy supply based on renewable energies, and has been closely monitored over a period of about 5 years [3]. The building has a measured heating demand of just over 30 kWh/(m^2 a), and the primary heat supply is from shallow geothermal energy in connection with two electrical brine/water heat pumps. An essential element of the monitoring is investigating the possibilities of a long-term, sustainable, energy efficient management and use of the geothermal field, whereby in principle both the heating and cooling (free cooling) of the building should be achieved from the ground.

Numerous studies have already fundamentally examined the various geothermal systems [4,5]. The use of geothermal systems as a heat source or heat sink, even for large buildings and correspondingly with higher performance, has also been examined in

* Corresponding author.
E-mail addresses: kristian.duus@tuhh.de (K. Duus), schmitz@tuhh.de (G. Schmitz).

https://doi.org/10.1016/j.enbuild.2021.110726
0378-7788/© 2021 The Authors. Published by Elsevier B.V.
This is an open access article under the CC BY license (http://creativecommons.org/licenses/by/4.0/).

Nomenclature

Symbols

APF	annual performance factor (–)
f	factor (–)
G	degree days (K d)
I	electric current (A)
λ	thermal conductivity (W/mK)
MAT	monthly average temperature (°C)
P	electrical power (kW)
Q	thermal energy (kWh)
$\dot{Q}$	thermal power (kW)
SPF	seasonal performance factor (–)
t	time (s)
U	heat transfer coefficient (W/m^2 K)
$\dot{V}$	volume flow (m^3/h)
ϑ	temperature (°C, K)
W	electrical energy (kWh)

Subscripts and abbreviations

a	annual
AEB	observation borehole outside of the energy pile field
AHU	air handling unit
B0/W35	brine 0 °C/water35 °C
DGNB	German Sustainable Building Council
DHW	domestic hot water
DTS	distributed temperature sensing
EB	observation borehole in the energy pile field
EER	energy efficiency ratio
EnOB	Energy-Optimized Building Construction
EP	energy pile
FC	free cooling
GHP	ground-coupled heat pump
in	inlet
LH	local heating
m	daytime average
max	maximum
min	minimum
mtf	mullion and transom façade
nom	nominal
OPC	Open Platform Communications
out	outlet
P	primary energy, circulating pump
PU	circulating pump
S	season
SEER	seasonal energy efficiency ratio
th	thermal
uf	unitised façade
use	useful

numerous studies [6–10]. Generally speaking, sustainable use of the ground via closed loop systems such as energy piles is not possible in the case of one-directional operation, i.e. with exclusive energy drain or exclusive energy feed, and thus an unbalanced annual energy input/output. According to Li et al. [11] for example, it was shown by simulation that the exclusive use of the ground for heating in combination with a heat pump reduces the soil temperature by around 6 °C within 5 years. Exclusive use of the ground for cooling in combination with a cooling system increases the soil temperature to over 35 °C within 13 years [11]. In both cases, the geothermal field is no longer usable – or can no longer be used efficiently – and this can also have a negative impact on the microorganisms in the soil. The combined use of the ground both as a heat source and a heat sink is therefore beneficial in this regard, and under the appropriate conditions (including no or only limited groundwater flow in the soil) can enable a sustainable and thus permanently energy efficient use of a geothermal field. However, in this regard it is crucially important to balance annual energy input/output as much as possible. According to Luo et al. [12], with a highly unbalanced annual energy input/output – in the case of a much higher energy withdrawal compared to energy input – over a period of 4 years, there is an average rise in the seasonal energy efficiency ratio (SEER) of free cooling of nearly 9% annually, whereas the annual performance factor of the heat pump decreases by about 4% annually.

The use of the ground as a combined heat source and heat sink has also been examined in various studies. Naicker and Rees [13] have conducted detailed studies of a large geothermal field consisting of 56 borehole heat exchangers for heating and cooling a university building using geothermal heating pumps. In doing so, their focus was on the efficiency of the heat pump operation. Decreases/increases in the ground temperature levels, both over shorter periods of several days as well as year-round, were significantly lower than expected, probably due to lower heating/cooling requirements of the building than originally assumed. The efficiency of heat pump respectively chiller operation proved to be satisfactory – but worse than expected. Cooling was found to dominate the energy demands compared to heating. This highlighted the importance already in the planning phase of a geothermal field of the availability of reliable and accurate data, inter alia on the heating and cooling needs of a building. Witte and Van Gelder [14] also investigated a geothermal probe field for heating and cooling an office building and warehouse using geothermal heat pumps. However their focus was, among other aspects, on investigating the possibility of targeted adjustment of the unbalanced annual energy input/output of the ground, based on the calculated higher cooling requirements of the building compared to its heating requirements. For this purpose, a heat exchanger for re-cooling was incorporated into the building's energy concept, which should provide relief for the geothermal probe field in the early spring months. In the course of the monitoring, the actual amount of energy input into the ground proved to be much higher than the amount of energy withdrawn from the ground, which resulted in a continuously increasing soil temperature level over the years of its operation. After the first three years of operation – with a corresponding trend in soil temperatures – it was planned to install the re-cooler. However, the building was closed down, the heat exchanger was not installed, and thus no corresponding data is available. Li et al., Dehghan and Bode et al. [15–17] have numerically investigated the topic of geothermal probe fields in connection with heat pumps for heating and cooling buildings. In doing so, Li et al. (2009) [15] focused on the imbalance between heat input into the ground and heat withdrawn from the ground, and the associated soil temperature distribution around the geothermal probes. The basis of the investigations is a three-dimensional FLUENT model. The results showed that the soil temperature increased around the geothermal probes, due to a surplus of energy input during the cooling period versus energy withdrawn during the heating period – which decreases the system performance and efficiency in cooling mode. In addition, they showed that this

imbalance can be resolved effectively by using a multi-functional ground-coupled heat pump with additional domestic hot water generation and thus in the long term, constant ground temperature levels can be achieved. Bode et al. [17] focused on the control of a building in conjunction with a complex heat pump system and geothermal probe field, whereby possibilities for mode-based control were investigated. This included optimising the combination of different load and supply cases. They were able to demonstrate that mode-based control enables the integration of renewable energies into a conventional energy concept.

In the context of this study, an exceptionally large geothermal field with approximately 950 energy piles consisting of double U-tube borehole heat exchangers with a depth of about 13 m each was investigated. Overall, the geothermal energy system comprises nearly 40 km of pipelines. In addition, the technical equipment and strategies of the energy concept for the building envisage and enable a targeted adjustment of the annual energy input/output for the soil in the geothermal field. As well as the fundamental heat withdrawal during the heating period for base-load supply of heating and domestic hot water systems, as well as the heat input during the cooling period for cooling the premises through thermoactive ceilings, there are high-performance re-coolers for further cooling or warming of the soil during the transitional periods. The building is therefore not cooled via the heat pumps used for the heat supply, but instead via free cooling. The monitoring of soil temperatures to assess the impact of geothermal energy use on the environment, as well as to assess the sustainability and energy efficiency of geothermal energy use, does not take place conventionally using thermistor chains, but instead by means of a fibre optic Distributed Temperature Sensing (DTS) system. This makes it possible in practice to determine the temperatures at any soil depth with a high level of accuracy. To date, the measures for targeted adjustment of energy input/output for the soil have been manually derived and implemented from the temperature curves. An appropriate automated control system should be investigated for this purpose, and implemented once adequately developed. A model predictive control of the building operation, taking into account the management of the geothermal field in terms of adjusting temperature levels in the soil, would be optimal regarding the sustainability and energy efficiency of the building's energy supply, and should be further investigated in future.

2. Office building

The office building, located in the city of Hamburg in northern Germany, and some of the main components of the technical installations are shown in Fig. 2.1. In total, the building consists of seven lower building sections (A–D & F–H) and one high-rise building section (E) which are interconnected by two building wings. The building wing consisting of sections A–D is oriented west and the building wing consisting of sections F–H is oriented north. Each of the lower sections has five floors; the high-rise building section has 13 floors, excluding basement areas and underground parking. The building envelope is basically realized as a unitised façade consisting of several mounted façade elements or it is partially realized as a mullion and transom façade. Furthermore, the external appearance of the building is characterized by the curved façade construction and horizontal coloured ceramic panels as shown in Fig. 2.1. The average heat transfer coefficient of the unitised façade is $U_{uf} = 0.87\ W/(m^2\ K)$, of the mullion and transom façade $U_{mtf} = 1.07\ W/(m^2\ K)$. Window-to-wall ratio of the entire building is 25% in case of solely considering the transparent share of the windows and surface-to-volume ratio is 0.2 m^2/m^3. The building was built within the framework of the research initiative "Energy-Optimized Building Construction" (EnOB), funded by the German government. Providing a net floor space of 46,500 m^2, the building contains space for around 1500 workplaces. The building was awarded the highest standard "Platin", formally "Gold", according to the German Sustainable Building Council (DGNB). Characterized as an energy efficient and sustainable building, the building was planned to achieve a primary energy demand of less than 70 kWh/(m^2 a) and a heating demand of maximum 15 kWh/(m^2 a). The objective concerning primary energy demand is achieved from the first year of operation on, the achieved heating demand is actual more than twice as high as the target value from the design stage. Nevertheless, a heating demand in the range of 30 kWh/(m^2 a) is excellent compared with other energy efficient buildings. The increased demand in operation phase has several causes, primarily different circumstances and conditions compared with planning like higher room temperature in order to increase user satisfaction, lower internal heat gains as presumed and not ideal user behaviour. The building is part of a local heating grid.

2.1. System description

The schematic layout of the thermal energy supply is shown in Fig. 2.2. Thermal energy is primary supplied by two ground-coupled heat pumps (nominal thermal power output each: $\dot{Q}_{GHP,nom} = 232$ kW at B0/W35) in parallel operation. A connection to the local heating grid "Energieverbund Wilhelmsburg Mitte" (nominal thermal power output $\dot{Q}_{LH,nom} = 750$ kW) is realized for domestic hot water (DHW) supply as well as to cover thermal peak loads of space heating supply. The local heating grid is based on a biomethane CHP plant with electrical output of 750 kW and thermal output of 370 kW in addition with two biomethane peak load boilers with thermal output of 1100 kW each. Since solely biomethane is used, the primary energy factor of the local heating is $f_p = 0.0$. The electrically driven ground-coupled heat pumps are connected to 950 energy piles within an energy pile plant below the building. Both systems feed a central warm water storage with a capacity of 5 m^3. During winter mode, the building is primarily heated using thermoactive ceilings in form of thermally activated

Fig. 2.1. Exterior view of the office building, part of the heating system and heat pumps.

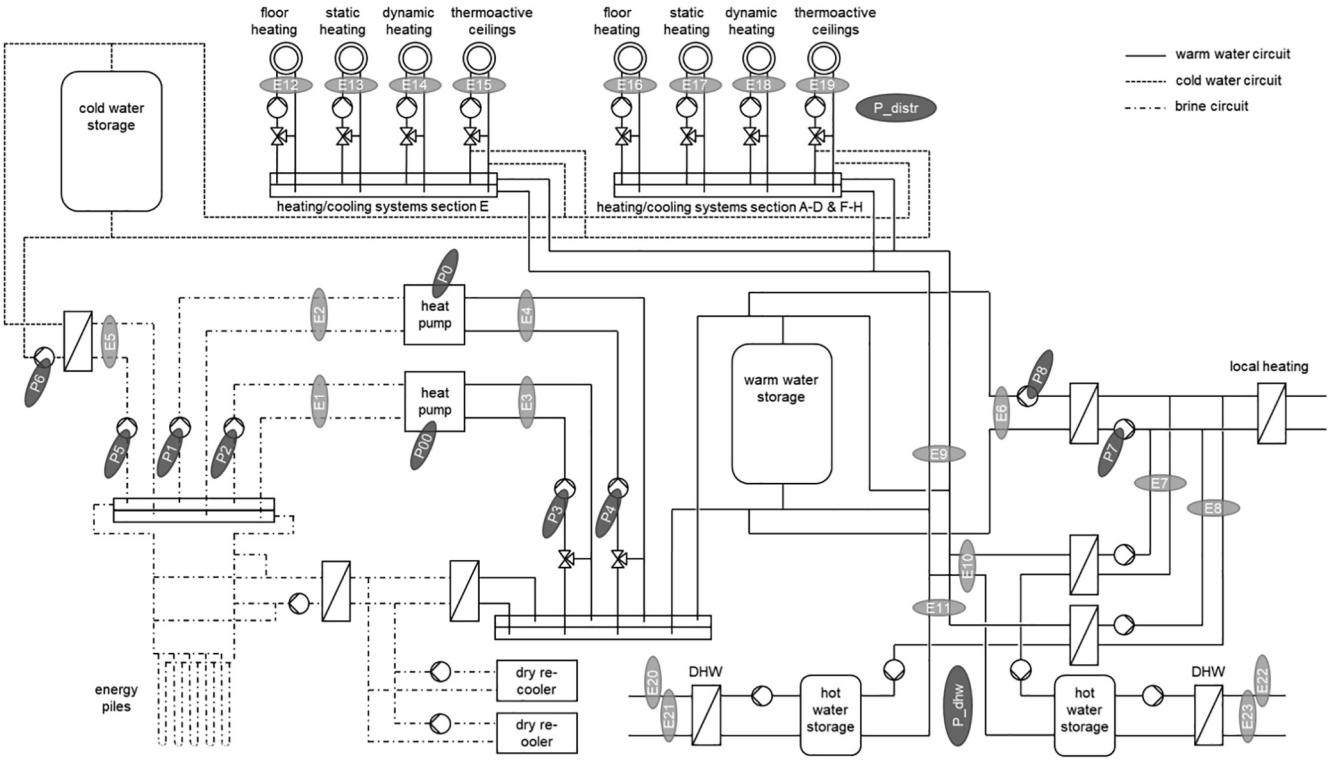

Fig. 2.2. System layout of the thermal energy supply with relevant heat meters marked E1...E23 and relevant electrical energy meters marked P00...P7, P_dhw (pumps for Domestic Hot Water supply), P_distr (distributor pumps of the heating/cooling systems).

concrete ceilings with a nominal design temperature of $\vartheta_{\mathrm{nom,in/out}} = 32\ ^{\circ}\mathrm{C}/28\ ^{\circ}\mathrm{C}$ for inlet respectively outlet temperature. This is mostly true for the office spaces. Other functional areas, e.g. corridors and basement areas, are heated using floor heating with a nominal design temperature of $\vartheta_{\mathrm{nom,in/out}} = 35\ ^{\circ}\mathrm{C}/28\ ^{\circ}\mathrm{C}$ or static heating with $\vartheta_{\mathrm{nom,in/out}} = 49\ ^{\circ}\mathrm{C}/28\ ^{\circ}\mathrm{C}$. In this case, static heating represents heating devices in form of radiators and convectors. In addition, dynamic heating is used to reheat processed air to the desired supply air temperature. If the building's heating demand cannot be covered by the GHP system alone, local heating is integrated into the warm water circuit as shown in Fig. 2.2. During summer mode, the building is cooled by free geothermal cooling. Another storage system of 5 m^3 is integrated into the cold water circuit to enlarge the energy storage capacity of the system. Generally, cooling buildings by using thermoactive ceilings enables the use of heat sinks operating on a higher temperature level compared to conventional cooling circuits. Therefor cold water with a temperature level in the range of 16 °C is sufficient. In this case, the nominal design temperature for the thermoactive ceilings in cooling mode is $\vartheta_{\mathrm{nom,in/out}} = 14\ ^{\circ}\mathrm{C}/22\ ^{\circ}\mathrm{C}$. The geothermal system is thus used efficiently throughout the year as a heat sink and heat source. With the exception of the thermoactive ceilings for cooling, other water circuits are not used for cooling during summer mode. To control the overall system fully automated in winter and summer operation modes, dynamic averaging of the outside air temperature for the past 36 h is used: the latest average outside air temperature is compared to the set points for winter and summer mode. Two dry re-cooling units can be used for cooling applications at appropriate outside air conditions as well as further cooling or warming of the geothermal field in order to purposefully adjust the thermal balance of the soil. Functional areas that are not associated to office space, e.g. utility, server and elevator machinery rooms, are conditioned throughout the whole year using conventional compression chiller split units.

The domestic hot water supply is ensured throughout the whole year. Central DHW as shown in Fig. 2.2 is provided for the canteen and changing rooms within the building, using separate domestic hot water stations. DHW within other functional areas, e.g. staff kitchens, is provided using decentral electrical instantaneous water heaters. The central DHW supply is based on the principle of instantaneous water heating as well. In winter mode, hot water for the DHW supply is preheated by the building's warm water circuit. It is reheated to the required hot water temperature within water to water heat exchangers supplied by local heating. During the summer when the GHP systems are not operated, the DHW supply is provided solely by thermal energy from the local heating system. Two additional hot water storage systems of 1.5 m^3 each are integrated into the warm water circuit in order to enlarge the system's thermal storage capacity. Domestic hot water is provided by downstream water to water heat exchangers.

Every building section is equipped with an air handling unit (AHU) for mechanical ventilation of the related office spaces and other functional areas. These are equipped with independent air handling units to cover the individual ventilation requirements of special functional areas like the canteen or the conference area. The ventilation concept is designed in accordance with the winter and summer modes of the building's entire energy concept. During winter mode, outside air is preheated by heat recovery within a cross-flow heat exchanger. If necessary, processed air is reheated to the desired supply air temperature (dynamic heating, see Fig. 2.2). Volume flows of supply and extract air are controlled to be constant at $3200 \cdots 32,000\ m^3/h$, depending on the floor space of the corresponding building section. During summer mode, the main AHU is not operated in general, whereby mechanical ventilation of sanitary areas is ensured by small ancillary ventilators as well. Ventilation of office areas is then replaced by manual ventilation using weather-proofed ventilation flaps integrated into the façade elements.

2.2. Geothermal system

Due to the present underground conditions, the building is founded on 1600 foundation piles. Around 950 of these foundation piles are designed as energy piles in form of double U-tube borehole heat exchangers (see Fig. 2.3), assembled in groups of usually ten energy piles (EP) using the Tichelmann principle. The geometric arrangement of the energy piles directly corresponds to the arrangement of the foundation piles due to static aspects. The distance between nearby energy piles is at least 3 m.

The undisturbed temperature of the soil in the region of the geothermal field was determined in a thermal response test conducted before the operational phase as 11 °C. The soil primarily consists of medium and coarse sand with a hydraulic conductivity in the range of 10^{-4}–10^{-2} m/s [18] up to a depth of 2 m below the ground surface. A layer of peat silt with a hydraulic conductivity in the range of 10^{-8}–10^{-6} m/s is located below this. The EPs in the remaining depth below 3 m are surrounded by fine, medium and coarse sand with a hydraulic conductivity in the range of 10^{-6}–10^{-2} m/s. The final drilling depth of the EPs is approximately 13 m; groundwater flows do not occur at the drilling location in general. A grouting material with improved thermal conductivity of$\lambda = 2.3\mathrm{W/(mK)}$ is used for thermal connection between EP ducting and surrounding soil. According to the conducted thermal response test, the surrounding soil has a surpassing effective thermal conductivity of $\lambda = 2.5\mathrm{W/(mK)}$.

The basic structure of the geothermal system is shown in Figs. 2.4 and 2.5.

The system consists of three main paths connected in parallel and merged in the heating centre of building sector E. Eleven energy pile distributors (V1–V11) with approx. six to ten groups of usually ten energy piles using the Tichelmann principle are connected to the three main paths in parallel to each other. The main path with energy pile distributors V1–V5 runs from the heating centre in building sector E parallel to the western building wing up to building sector A (see also Fig. 2.6). The main path with energy pile distributors V6 to V10 runs from the heating centre parallel to the northern building wing up to building sector H. The third main paths solely consists of energy pile distributor V11 located under building sector E.

2.3. Measurement devices and data acquisition

Relevant parameters characterizing the status of working fluids within the different subsystems are measured and recorded (Table 2.1). Each hydraulic circuit is evaluated by measuring the volume flow and fluid temperature at the inlet and outlet. Electrical energy demands of the relevant components (e.g. heat pumps, fans, circulating pumps) are measured as well. Referring to Fig. 2.3, an optical fibre cable is integrated into selected energy piles for site-resolved temperature measurements within the soil respectively the concrete, according to the principle of Distributed Temperature Sensing (DTS). 17 energy piles in total are equipped with temperature sensing. Additional 13 by this means monitored observation boreholes within and outside the energy pile plant are used to analyse the impact of geothermal energy provision on the surrounding soil as reference piles. A specific evaluation unit is installed to provide measured temperatures with a spatial resolution of approximately 1 m and a time resolution of 1 h. Fig. 2.6 depicts the layout of the building with localisation of the 17 monitored energy piles (designation: F… and G…) as well as the 8 observation boreholes in the energy pile field (designation: EB1–EB8) and the 5 observation boreholes outside of the energy pile field (designation: AEB1–AEB5). The outside observation boreholes are required for the DGNB certification in order to monitor the effects of the geothermal use on the environment and to be able to investigate and evaluate the surrounding soil.

All other relevant measurement signals are recorded every minute with the help of a LabVIEW programme which is used as OPC client. A Honeywell controlling system is used to control and regulate the overall system in general.

2.4. Climatic conditions

As essential background information with respect to interpretation and discussion of the following investigations, the climatic conditions in terms of degree days (G) and monthly average temperature (MAT) of the three years of operation and monitoring are shown in Fig. 2.7.

In this case, degree days based on average room temperature of 20 °C and heating threshold temperature of 15 °C are used and calculated in accordance with VDI 3807 [19] as follows:

$$G = (20\ ^{\circ}\mathrm{C} - \vartheta_{\mathrm{m}})\,1\mathrm{d}$$

with

G degree day in K d,
ϑ_{m} daytime average of outdoor temperature during one heating day ($\vartheta_{\mathrm{m}} < 15\ ^{\circ}\mathrm{C}$).

The sum over one calender month are the monthly degree days, over one calender year the annual degree days. In Table 2.2 the annual degree days for the three considered years are listed.

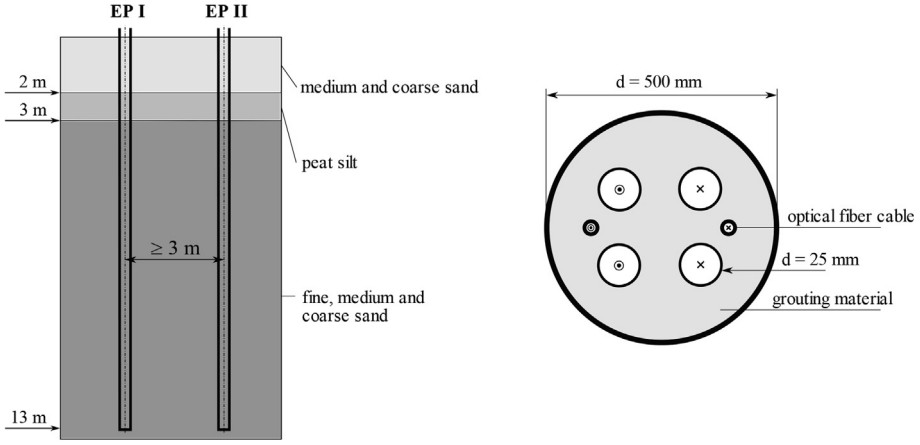

Fig. 2.3. Structure of the soil and energy piles.

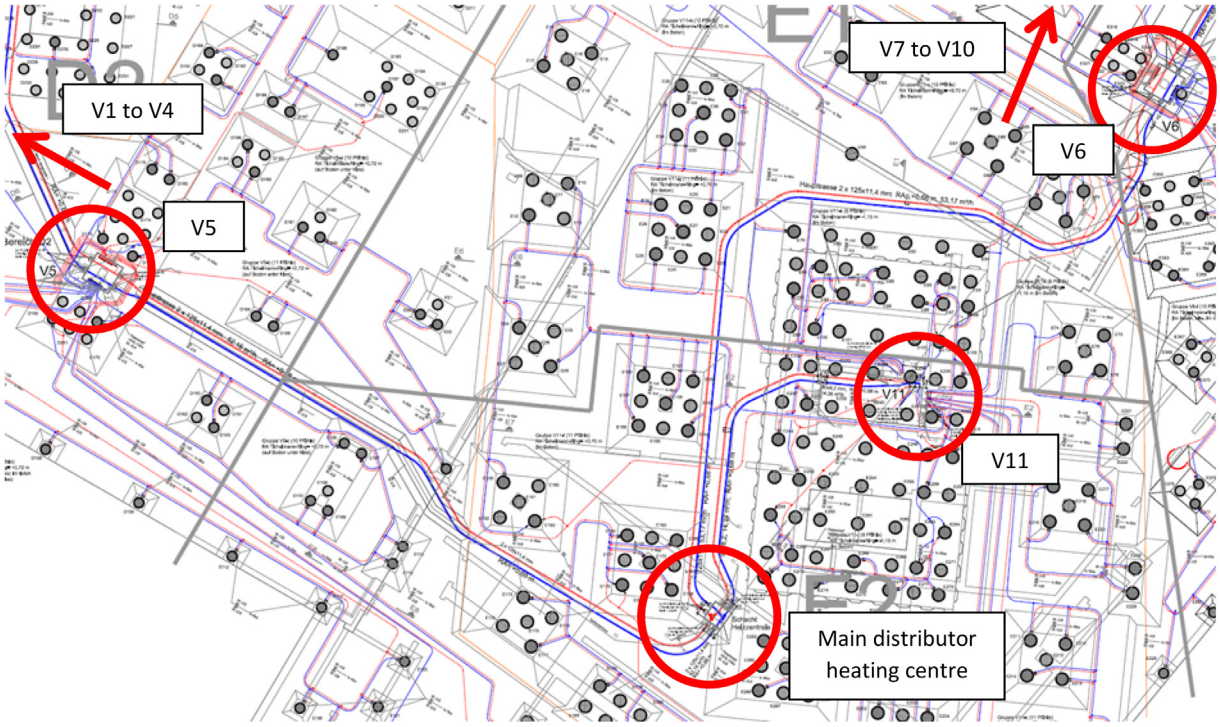

Fig. 2.4. Schematic depiction of the basic structure of the geothermal system regarding setup and arrangement of the energy pile distributors (V1–V11); energy piles shown in dark grey filled circles, foundation piles shown in light grey filled circles.

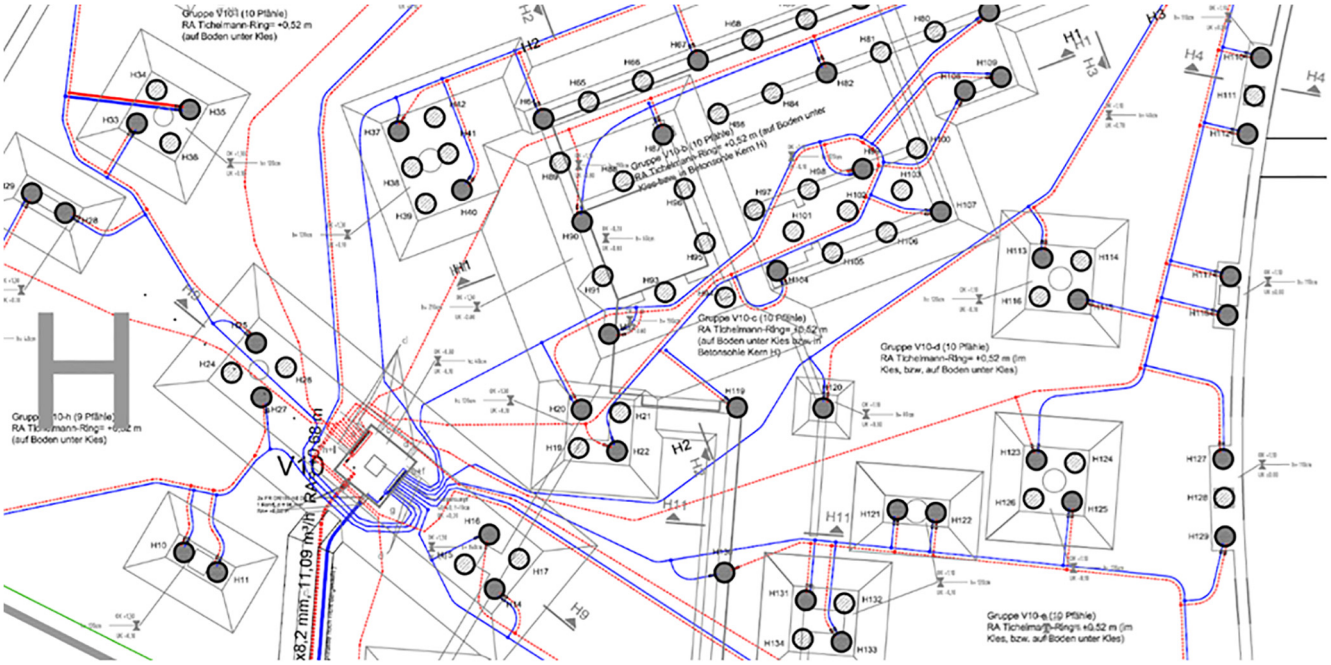

Fig. 2.5. Schematic depiction of energy pile distributor V10 regarding arrangement of the energy pile groups as well as the single energy piles within the different groups; energy piles shown in dark grey filled circles, foundation piles shown in light grey filled circles.

As it can be seen in Fig. 2.7 as well as Table 2.2, the climatic conditions of the three considered years are very similar, in terms of both degree days and monthly average temperature. Apparent differences can only be seen during summertime in May, June and September as well as during wintertime in November and December. Compared to the reference year, the three considered years of monitoring are in terms of outdoor temperature above average.

3. Monitoring results

The results presented in this study are based on measured data of the building operation from January 2014 till December 2017.

The following evaluation is subdivided into two parts. First, the relevant thermal and electrical energy demands during winter and summer operation are presented and analysed. Afterwards, the

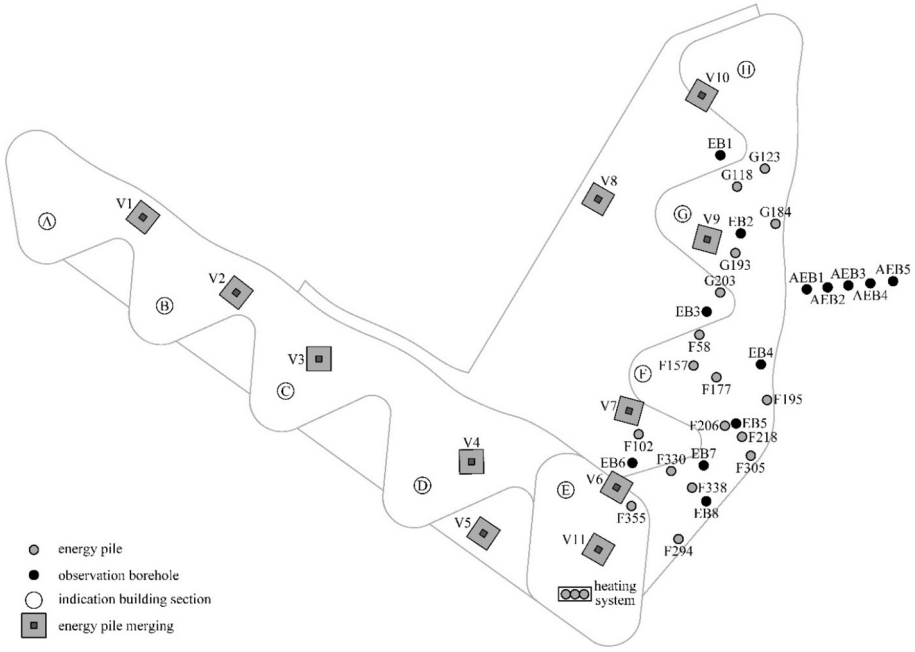

Fig. 2.6. Schematic depiction of the layout of the building with localisation of the 17 monitored energy piles as well as the 8 observation boreholes in the energy pile field and the 5 observation boreholes outside of the energy pile field.

Table 2.1
Measurement devices and related measurement uncertainties.

Measured value		Sensor type/ measuring principle	Measurement uncertainty
Temperature (water)	ϑ	Pt500 resistance thermometer	$\pm(0.5+3\cdot(\Delta\vartheta_{min}/\Delta\vartheta))\%$ with $3\ K<\Delta\vartheta<150\ K$
Temperature (soil)	ϑ	Optical transmission system	±0.2 K
Volume flow (water)	$\dot{V}$	Impeller flow meter	$\pm\left(2+0.02\cdot\left(\dot{V}_{max}/\dot{V}\right)\right)\%$ of read., but $\leq 5\%$ of reading
Thermal energy	Q	Heat meter	$\pm6\%$ of reading
Electrical energy	W	AC energy meter	$\pm1\%$ of reading for $I>100$ mA, else $\pm2\%$ofreading

temperature profiles of observation boreholes and energy piles in conjunction with thermal energy balances of the soil are shown and discussed with respect to sustainability and energy efficiency.

3.1. Thermal and electrical energy demands

Figs. 3.1 and 3.2 respectively depict the flow charts of the heating and cooling operations for the whole of 2016. The charts provide a clear overview of the distribution of the total energy consumption for a year of operation. 2016 is taken as benchmark year for system operation because it is the first complete year of operation after initial adjustment process and so can be considered as a reference year. In addition, 2016 is the year of operation with the most extensive measurement data.

Fig. 3.1 shows that by far the largest thermal energy demand is for the thermoactive ceiling heating system, through which all the office areas are heated. Another large component of thermal energy demands is the dynamic heating system. This is the thermal energy transferred to the incoming air supply, after it has already been preheated via heat recovery, in order to attain the required supply air temperature. The systems of static heating and underfloor heating are only used in special areas, and therefore only constitute a small percentage of the total energy demand. The flow chart confirms the basic heating strategy in form of primary supplying thermal energy by the two ground-coupled heat pumps and solely additionally using local heating connection to cover

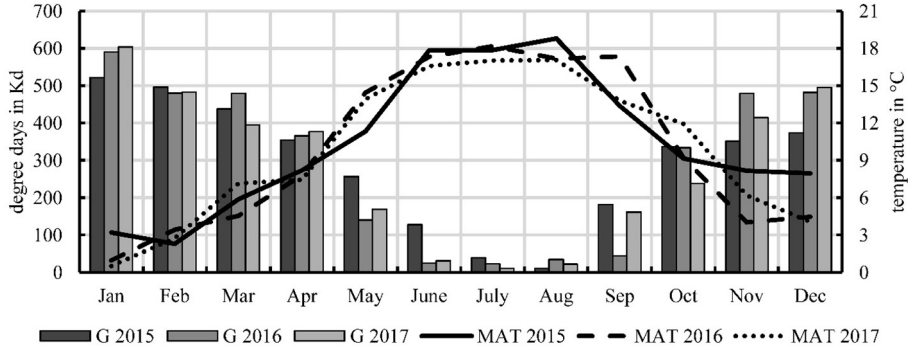

Fig. 2.7. Climatic conditions of the three years of operation and monitoring in terms of degree days (G) and monthly average temperature (MAT).

Table 2.2
Annual degree days G_a for Hamburg-Fuhlsbüttel and the years of operation 2015–2017 as well as the reference year.

Period			G_a in (K d)/a
January 2015	to	December 2015	3484
January 2016	to	December 2016	3478
January 2017	to	December 2017	3398
Reference year (long-term average, 1971–2017)			3755

thermal peak loads as well as for domestic hot water supply. The share of local heating on the total energy supply is about 27%. Inconsistencies in the individual totals regarding missing energy quantities (e.g. meter E9 compared with the sum of meters in the heating circuits) are treated as losses, as well as being attributed to measurement uncertainties.

Fig. 3.2 shows that for cooling, building section E with its share of approx. 43% has nearly the same energy demands for cooling the office areas as all the other building sections together.

The basic design of the energy concept can also be seen. In 2016, for the main part of the building a total of 479.4 MWh thermal energy and 9.0 MWh electrical energy were used to cool the building (free cooling through the soil). Even if there is a further electrical energy demand of 105.2 MWh for the split units conditioning special functional areas, primarily cooling mechanisms that are not based on compression chillers were used.

The 2016 annual performance factors (APF) of the two heat pumps, as well as the seasonal performance factor (SPF) for free cooling, can be derived directly from Figs. 3.1 and 3.2. The annual performance factor for the evaluation of the heat pump operation is given by the ratio of the useful heat output to the electrical energy demand of the heat pump system as well as the energy demand of the central circulating pumps,

$$\mathrm{APF_{GHP}} = \frac{\int \dot{Q}_{\mathrm{GHP}} \mathrm{d}t}{\int (P_{\mathrm{GHP}} + P_{\mathrm{PU}}) \mathrm{d}t}.$$

Similar to the evaluation of the heat pumps, a seasonal performance factor is determined for the evaluation of free cooling through the soil,

$$\mathrm{SPF_{FC}} = \frac{\int_S \dot{Q}_{\mathrm{FC}}\, \mathrm{d}t}{\int_S P_{\mathrm{PU}}\, \mathrm{d}t}$$

The $\mathrm{SPF_{FC}}$ measures the benefits gained by transferring thermal energy from the building into the ground, in relation to the energy demand of the required central circulating pumps. Table 3.1 summarises the values for all years of operation for which corresponding measurement data is available. SPF is missing for the years 2014 and 2015 due to missing measurement data in terms of not separated electrical energy demands of the circulating pumps P5 and P6. The circulating pumps P5 and P6 were only measured together in the beginning of the monitoring. In addition to the performance factors that address the heat pumps only, the performance factors of the heat pumps also including the electrical energy demand of

a. the circulating pumps of the geothermal field (P1 and P2),
b. the circulating pumps of the geothermal field (P1 and P2) and the central circulating pumps of the warm water circuit (P3 and P4)

are listed. In addition to the performance factor for free cooling that addresses the circulating pump of the geothermal field (P5) only, the performance factor for free cooling that also includes the electrical energy demand of the central circulating pump of the cold water circuit (P6) is listed as well.

The annual performance factors of the two heat pumps without taking into account the circulating pumps could be steadily increased over the years by undertaking several optimisation measures, whereby in total the APF of heat pump 1 increased by approximately 12.5%, and the APF of heat pump 2 by approximately 16%.

One effective measure was a change of the basic control strategy regarding the warm water storage from single-point control strategy to double-point control strategy. Due to the resulting improved usage of the storage capacity, the operation phases of the heat pumps were extended and a massive cyclic operation was avoided. Moreover, a change of the control strategy for domestic hot water supply has improved the heat pump operation. The initial strategy to switch on the heat pumps with high temperature set point (50 °C) in cases of domestic hot water requirement was eliminated, so that the heat pumps solely indirectly cover the base load for domestic hot water supply with low temperature level according to the actual given set point of the heating system. The reduced temperature lift of the heat pump process also led to a more efficient heat pump operation. Including the electrical energy demand of the central circulating pumps into APF evaluation shows that the primary pumps (geothermal field) have much more negative impact on the APF compared to the secondary circulating pumps (warm water circuit). If you consider the two years of 2016 and 2017, the free cooling without taking into account the secondary circulating pump shows a significant drop in the seasonal performance factor (−47%). The reason for this is a significantly

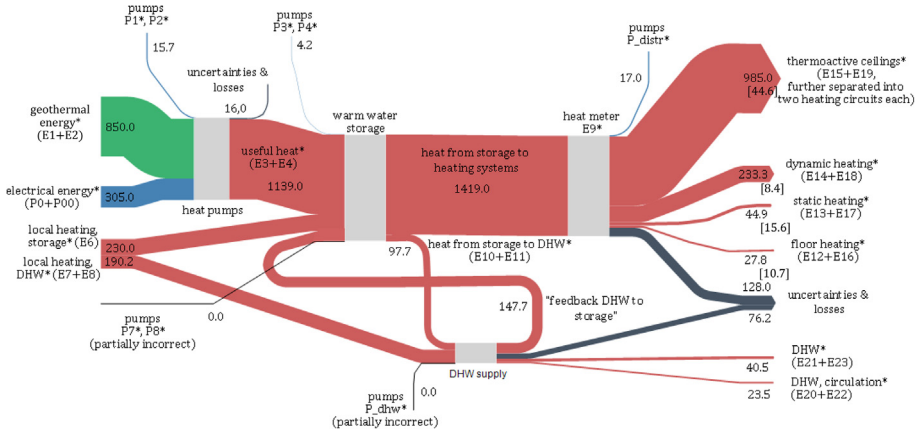

Fig. 3.1. Flow chart of the heating operations for the year 2016, all energy quantities are given in MWh, energy demands per net heated floor area are given in kWh/m^2 and listed in square brackets; energy quantities marked with * are measured directly, the respective meters taken into account are labelled E1…E23 for heat meters and P00…P7, P_dhw and P_distr for electrical energy meters (see Fig. 2.2).

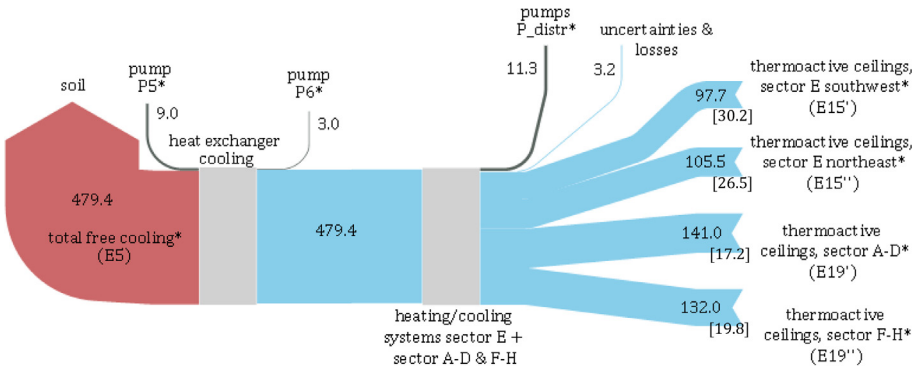

Fig. 3.2. Flow chart of the cooling operations for the year 2016, all energy quantities are given in MWh, energy demands per net heated floor area are given in kWh/m^2 and listed in square brackets; energy quantities marked with * are measured directly, the respective meters taken into account are labelled E1...E23 for heat meters and P00...P7, P_dhw and P_distr for electrical energy meters (see Fig. 2.2).

Table 3.1
Annual performance factors (APF) of the two heat pump (GHP) systems and seasonal performance factor (SPF) of the free cooling for the years of operation 2014 to 2017; GHP1 and GHP2: solely electrical energy demand of heat pump, +P1 and +P2: electrical energy demand of heat pump plus primary circulating pump, +P2,P3 and +P1,P4: electrical energy demand of heat pump plus primary and secondary circulating pump; free cooling, P5: solely electrical energy demand of primary circulating pump, +P6: electrical energy demand of primary and secondary circulating pump; for circulating pump notation see Fig. 2.2.

Year of operation	APF GHP1 [–]			APF GHP2 [–]			SPF Free cooling [–]	
	GHP1	+P2	+P2,P3	GHP2	+P1	+P1,P4	P5	+P6
2014	3.28	3.12	3.09	3.33	3.18	3.14	–	–
2015	3.26	3.17	3.14	3.35	3.24	3.22	–	–
2016	3.66	3.45	3.40	3.81	3.66	3.62	53.02	39.78
2017	3.69	3.45	3.39	3.86	3.74	3.70	28.11	23.98

increased power demand for the geothermal energy circulating pump (P5) in 2017. Increasing the performance of the geothermal energy circulating pump (P5) at the end of the 2016 cooling period was an intended measure to improve the brine flow through the geothermal system. By use of ultrasonic flow measurement and further temperature profiles of energy piles, an inhomogeneous flow through the geothermal system was found. Generally speaking, energy piles connected to distributors which are close to the heating centre, meaning energy piles with minor pressure drops in the feed and return line, had shown a much higher flow than energy piles connected to distributors which are far from the heating centre, meaning energy piles with major pressure drops in the feed and return line. Hydraulic adjustment was not possible, because of insufficient performance of the circulating pump. Increasing the performance of the geothermal energy circulating pump has improved this issue, but did not fix it. Corresponding evaluations of this problem suggest that it is no dimensioning fault but rather due to higher pressure drops indeed compared to calculation.

3.2. Sustainable and energy efficient management of the geothermal field

A total of 17 energy piles and 13 observation boreholes were equipped with a fibre optic distributed temperature sensing (DTS) system, so that continuous temperature profiles can be recorded at different depths. Temperature profiles were specifically recorded for (see Fig. 2.6)

- 17 thermally activated foundation piles (designation: F... and G...) with a depth of 13 m,
- 8 observation boreholes in the energy pile field (designation: EB1–EB8) with a depth of 20 m,
- 5 observation boreholes outside of the energy pile field (designation: AEB1–AEB5) with a depth of 25 m.

The geological conditions in the area of the energy pile field are very homogeneous at the relevant depths (c.f. Section 2.2). There are no groundwater flows, which in principle enables the ground to be used for massive long-term storage, with heat input in summer and heat withdrawal in winter.

Fig. 3.3 shows the long-term temperature patterns of the observation borehole AEB5 outside the field at different depths with a time resolution of 1 h. The AEB5 observation borehole is located orthogonally at a distance of 15 m to the edge of the energy pile field. Due to gaps in the measurements, no temperature data is available – for the inside and outside observation boreholes as well as for the energy piles – for the period in April/May 2016 and for the three shorter periods in March and September 2016 and November 2017. The outside observation boreholes (AEB1–AEB5) are essentially for the assessment of geothermal energy use in terms of its impact on the environment. They enable potential long-term reductions or increases in the temperatures of the surrounding soil to be recorded, which may occur as a result of unbalanced management of the geothermal field, thereby enabling appropriate measures to counteract further cooling or warming to be implemented. In addition, temperature monitoring of the surrounding soil is also an important aspect of the German Sustainable Building Council (DGNB) certification.

While the top two layers of soil still exhibit a strong dependence on the outside temperature and thus the season, this influence decreases with increasing depth. From a depth of about 10 m, there are only slight temperature changes in the soil over the course of the year, which at the deepest layers are only minimal at approximately 0.25 K. Overall, the maximum and minimum temperatures in the soil are slightly delayed compared to the season, due to the slow heat conduction processes, whereby the time delay increases with increasing depth. Based on the fact that the temperature levels of the individual deeper-lying layers show almost no changes over the three years of operation and measurement (comparison 01.01.2015 – 01.01.2018), and are also close to

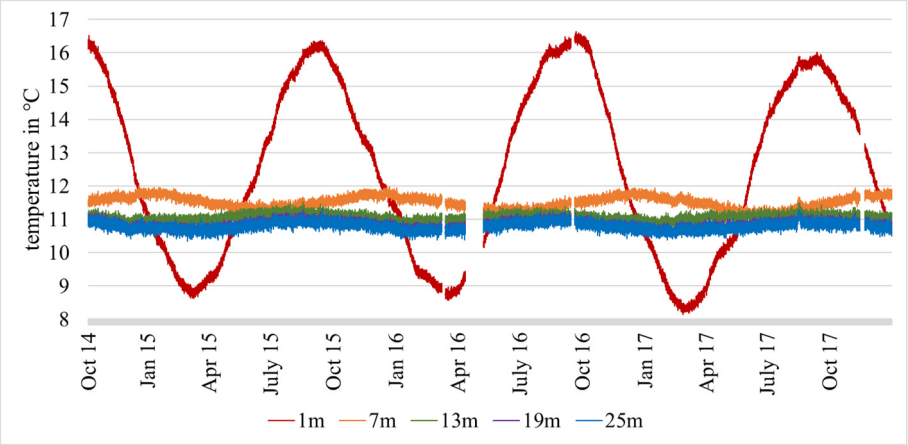

Fig. 3.3. Long-term temperature patterns at different depths for the outside observation borehole AEB5 for the period from October 2014 to December 2017.

the undisturbed temperature of 11 °C determined in a thermal response test conducted before the operational phase, the surrounding soil can currently be considered as undisturbed.

Fig. 3.4 shows the long-term temperature patterns of the observation borehole EB4 inside the energy pile field at different depths with a time resolution of 1 h.

As expected, the observation boreholes inside the energy pile field show greater temperature changes in the deeper layers in comparison to the outside observation boreholes. There is a significant, time-delayed and seasonally-affected (i.e. influenced by the outside temperature) impact on the soil temperature in the energy pile field, due to the summer heat input and the winter heat withdrawal. The soil temperature in the deepest layers in the region of observation borehole EB4 varies over the three years of operation between approx. 10.5 °C in summer mode and 11.0 °C in winter mode. What is striking is that the amplitudes of the temperature curves exhibit some significant variation, both in comparison between heating and cooling mode, as well as in terms of the individual years of operation. In addition, a kind of reversal can be noted in the period of June/July 2016, from a tendency towards decreasing temperatures to increasing temperatures. The main reason for this is a change made to the mode of operation of the technical systems, in particular during the cooling phase with the effect of an increasing heat input into the ground. Further information about these measures are given in the context of Fig. 3.6. If the temperatures occurring at the beginning of the measurements are compared with those at the end (c.f. 01.01.2015 and 01.01.2018), almost the same temperature levels can be identified in the lower-lying layers. This means that over the three years of operation, despite temporarily increased or decreased temperature levels occurring within the individual years due to the direct influence of heat input and withdrawal, an overall sustainable management of the energy pile field has ensured that ultimately the original temperatures of just over 11 °C have been achieved again.

Fig. 3.5 shows the long-term temperature patterns of the energy pile F305 at different depths with a time resolution of 1 h.

As can clearly be seen, the energy piles exhibit fundamentally very different dynamic temperature patterns to the observation boreholes. The outside temperature-dependent heating and cooling load profiles of the building can be clearly identified in the daily and weekly history, as well as the regeneration cycles during the course of the day and over the weekends. The fundamentally different temperature patterns between on the one hand energy piles as shown in Fig. 3.5 and on the other hand observation boreholes as shown in Figs. 3.3 and 3.4 result from the active part of the energy piles in terms of heat transfer between building and ground in contrast to the passive part of observations boreholes which are solely boreholes equipped with an optical fibre cable for measurement purposes and filled with a grouting material. The observation boreholes simply behave like the surrounding soil regarding heat transfer. The temperature level available for heating, respectively cooling purposes decreased from approx. 12 °C – 4 °C during winter mode and increased from approx. 9 °C – 18 °C during summer mode.

The maximum respectively minimum expected temperatures in the ground are temporarily nearly reached at the end of cooling

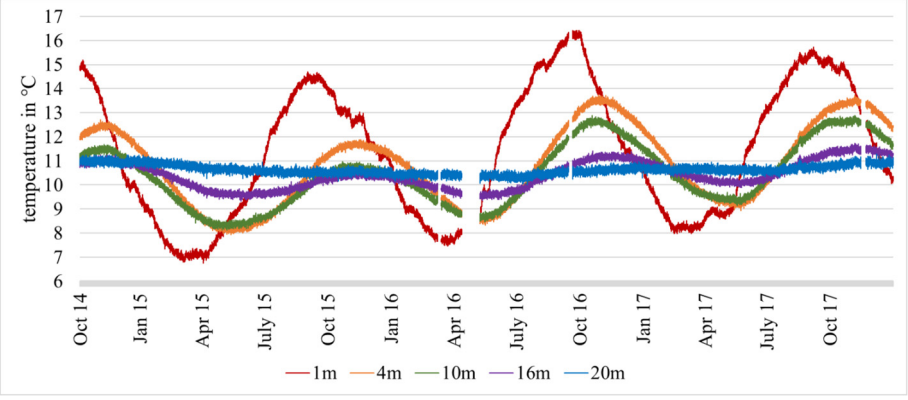

Fig. 3.4. Long-term temperature patterns at different depths for the inside observation borehole EB4 for the period from October 2014 to December 2017.

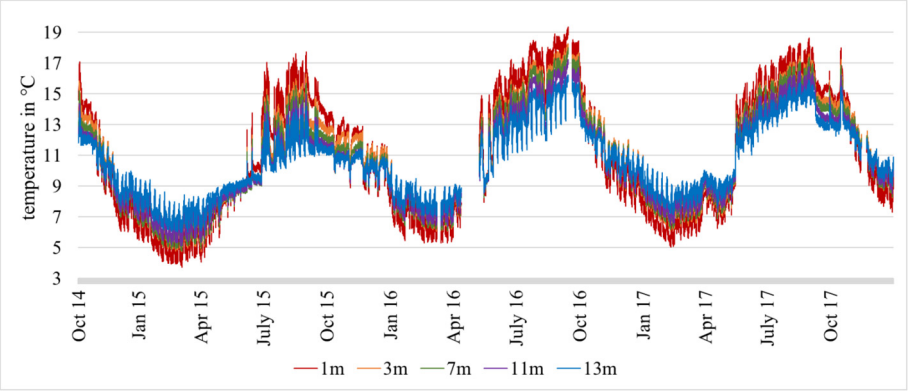

Fig. 3.5. Long-term temperature patterns at different depths for the energy pile F305 for the period from October 2014 to December 2017.

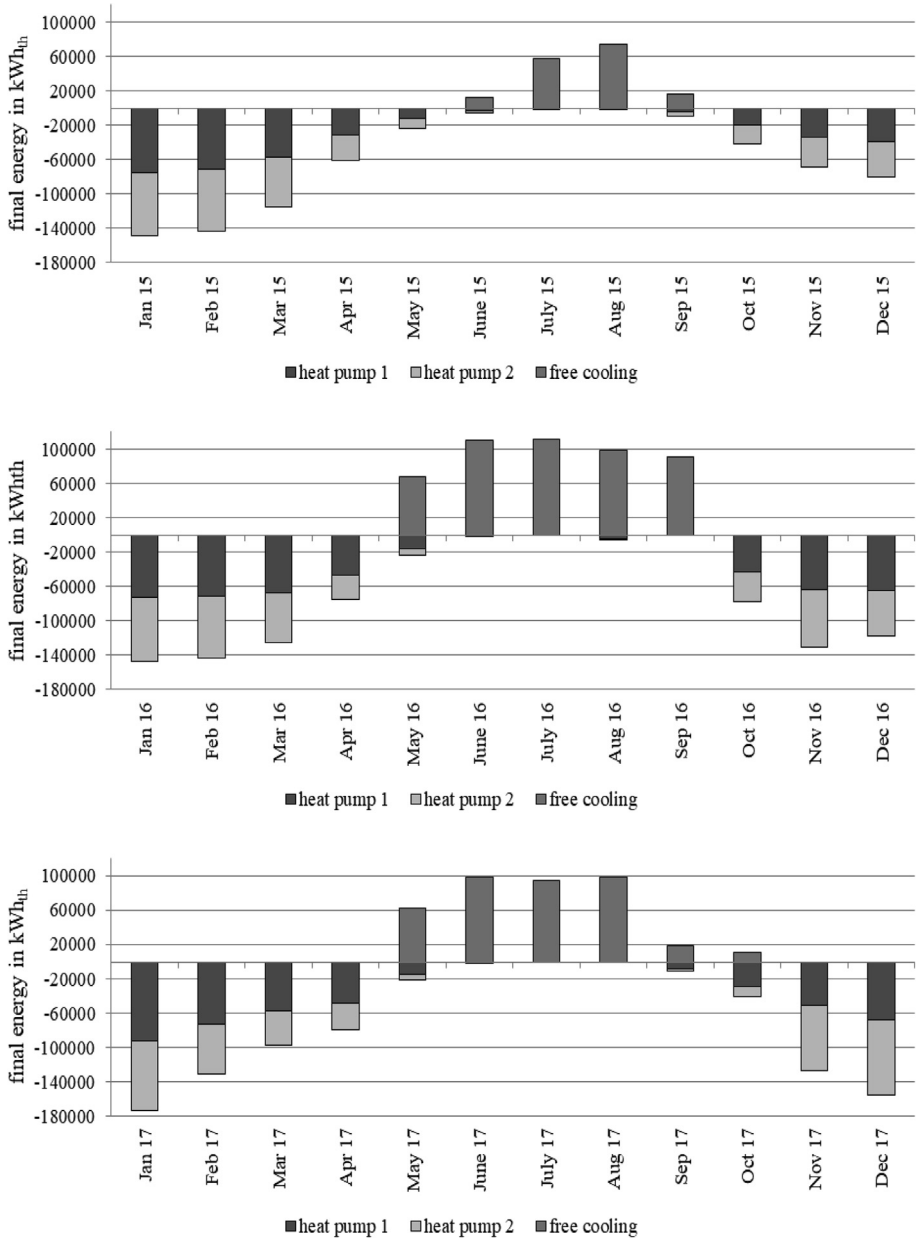

Fig. 3.6. Annual energy balance of the ground for the years of operation 2015 through 2017.

and heating period. This is true with regard to the heating and cooling system in terms of the solely direct usable section of the ground near the energy piles (due to the slow heat conduction processes). As mentioned, the available temperature level for heating respectively cooling decreases to approx. 4 °C during winter mode and increases to approx. 18 °C during summer mode. In the geothermal field with distance to the energy piles, the temperature remains on the level of the undisturbed temperature due to the targeted adjustment of the energy balance of the ground.

Sustainable management of the geothermal field – and thus reaching a balanced annual energy input/output for the soil – is of crucial importance for the sustainable and energy efficient heating and cooling of the building. Taking into account the fundamental building operating conditions, the sum of the heat input during the cooling period and the natural regeneration of the ground should mirror the heat withdrawal during the heating period as accurately as possible. This can prevent both long-term excessive warming as well as long-term excessive cooling of the soil in the geothermal field. As already mentioned above, a closer examination of the long-term temperature patterns of EB4 (Fig. 3.4) reveals a kind of reversal in the temperature conditions during the period of June/July 2016, from a tendency towards decreasing temperatures to increasing temperatures. The reason for this is the targeted expansion – both in terms of time as well as intensity – of the cooling operations (with a resulting positive effect on user comfort), and thus an increase in the heat input into the ground during the 2016 cooling period. Fig. 3.6 shows the annual energy balance of the ground in the form of monthly heat input as well as withdrawal for the years 2015 – 2017. The year 2014 is not included due to incomplete data.

When comparing 2015 with 2016 and 2017, there is similar heat withdrawal during the winter months, but drastically increased heat input in the summer months. Table 3.2 shows the summed monthly energy withdrawal from the ground as well as the summed monthly energy input into the ground for the years of monitoring. The total annual energy withdrawal from the ground only varies by about 20%, whereas the total annual energy input into the ground was actively increased by 201% comparing 2015 and 2016.

Between 2016 and 2017, no further changes were made to the free cooling, and the very low heat input especially noticeable in September 2017 compared with the previous year is due to different weather conditions.

Fig. 3.7 once again depicts the annual energy balance of the ground for the year 2016 in the form of monthly heat input as well as withdrawal, but in direct connection with the long-term temperature patterns of the energy pile F305 as well as the observation borehole EB4 inside the energy pile field.

Considering the three diagrams of Fig. 3.7 in turn beginning with the top, it can be seen as a kind of chronological sequence regarding the energy transfer shown by the time-delayed effects on the temperature profiles. The annual energy balance shows the amounts of heat transferred to the heat pumps and the cooling heat exchanger. With a closer alignment of the time axes of the diagrams, so that the respective time points of all charts fit together, it is evident that the energy transferred from/to the geothermal circuit arrives directly in the energy piles, and can be measured. However, it takes some time to transfer this amount of energy from the energy piles to the surrounding soil, depending on the distance of the point in the ground to the energy piles, due to the slow heat conduction processes. Using the example of the observation borehole EB4, located towards the edge of the geothermal field, there is an approximately one month delay in the temperature response of the soil. However, the crucial factor is ultimately the fact that due to the summer heat input, the soil temperature can be raised effectively in the geothermal field. As can be seen from the long-term temperature patterns in the ground over several years (Fig. 3.4 for EB4), the nature of operation of the cooling system in the summer months has a significant effect on the temperature levels occurring in the soil. Nevertheless, user comfort is a limiting factor which must be taken into account. Even though the expansion of the cooling operations undertaken in 2016 improved user comfort through lower room temperatures, a further expansion of the cooling system to enhance user comfort seems to only be of limited use. A further increase of cooling the office rooms in order to heat up the soil can result in decreasing user comfort due to too low room temperatures and/or too high temperature differences between inside and outside air. For example, several studies show, that temperature differences between inside and outside air should not exceed about 5 °C. For this reason, a type of portfolio should be created for the targeted adjustment of the energy balance of the ground, which could contain the following components:

- adjustment of the cooling system with a reduction or increase in cooling the office areas of the building, and thus the corresponding variation of the heat input into the ground, whereby the effect on user comfort is an important factor to be taken into account,
- adjustment of the heat supply with respect to the shares of geothermal energy and local heating, whereby economic aspects must also be considered here,
- the use of heat exchangers (re-coolers) for additional cooling of the soil during the spring months after a mild heating season, as envisaged in the planning of the building,
- and also the use of heat exchangers (re-coolers) for additional warming of the soil during the autumn months, possibly supplemented by a solar thermal system for even better performance and increased efficiency.

To date, all measures for adjustment of the operations have been implemented manually. Automated control of the building operation, taking into account the management of the geothermal field in terms of adjusting temperature levels in the soil, is necessary in future for the sustainability and energy efficiency of the building's energy supply. A model predictive control would be optimal.

Retrofitting a solar thermal system would be useful in several respects. For example, at the end of the cooling period, additional energy could be input into the ground, to boost the soil temperature and thereby increase the efficiency of the subsequent heating operations. In addition, during the actual heating operations, when

Table 3.2
Total energy withdrawal from the ground and total energy input into the ground for the several years of monitoring.

Year of operation	Energy withdrawal			Energy input		
	Monthly peak load [MWh]	Total [MWh]	Total increase compared to 2015 [%]	Monthly peak load [MWh]	Total [MWh]	Total increase compared to 2015 [%]
2015	148.6	700.0	–	74.1	159.4	–
2016	147.6	849.9	21	111.5	479.4	201
2017	173.2	835.4	19	98.7	383.8	141

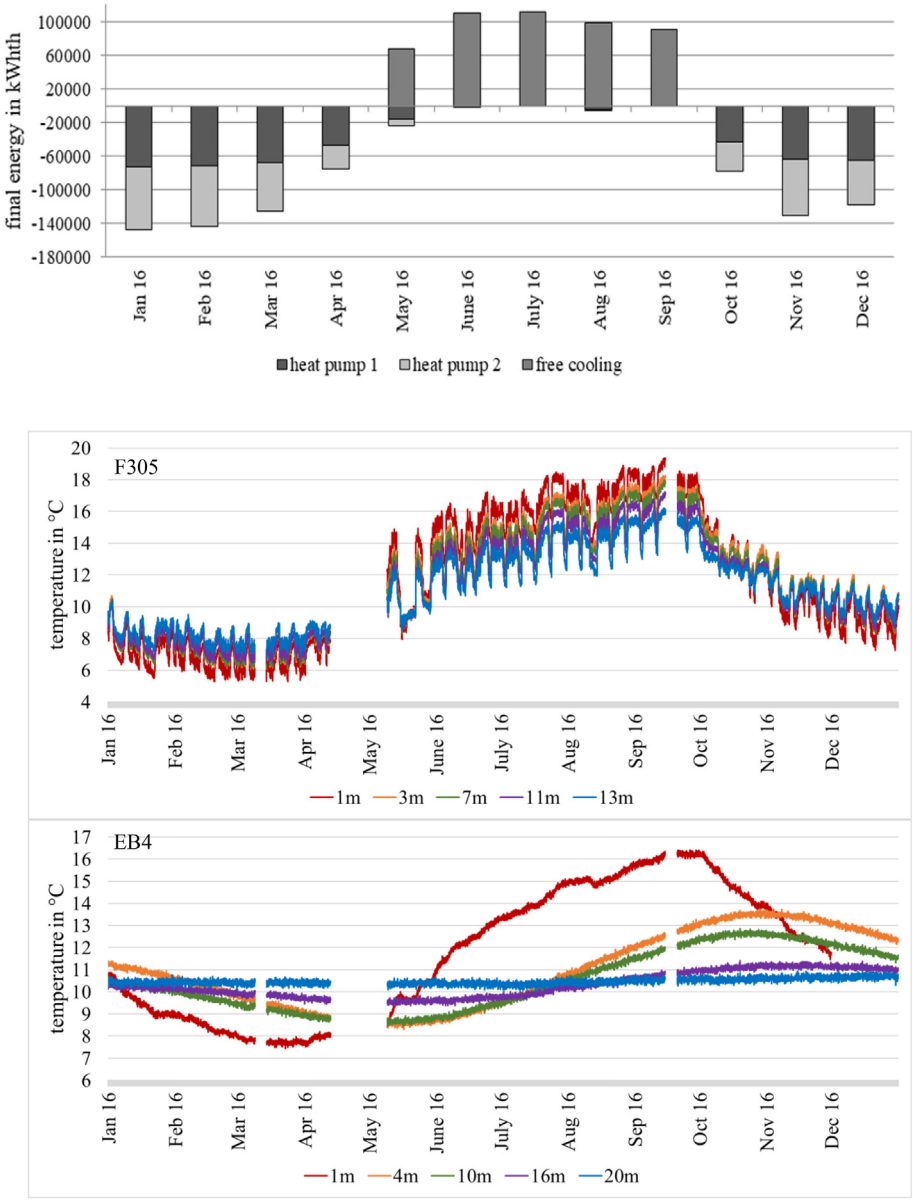

Fig. 3.7. Annual energy balance of the ground for the year 2016, in direct connection with the long-term temperature patterns of the energy pile F305 as well as the observation borehole EB4 inside the energy pile field.

the sun is shining solar energy could be used to heat up the incoming brine before it reaches the heat pumps, thereby also increasing the heat pump operating efficiency. In the summer, and insofar as possible also in winter, the solar energy could be used for domestic hot water generation.

4. Conclusions

This study investigated a large office building in terms of the efficient and sustainable use of the ground for thermal energy storage. During heating mode, the base load coverage for heating and hot water is provided by shallow geothermal energy, in combination with two electrical brine/water heat pumps, and local heating is used for peak load coverage or to reach the required temperature levels. In cooling mode, primarily cooling mechanisms that are not based on compression chillers are used for cooling the building (free cooling through the soil). The findings demonstrated that the annual performance factors of the heat pumps could be increased continuously over the years of operation by implementing optimisation measures, from 3.28 to 3.69 and 3.33 to 3.86. The seasonal performance factor of the free cooling decreased significantly from 2016 to 2017 due to the modified operating conditions, from 53.02 to 28.11.

With regard to the impact of geothermal energy use on the environment, the surrounding soil may currently be considered as undisturbed, based on the fibre optic distributed temperature sensing (DTS) system measurements. The ground temperature measurements within the geothermal field clearly show that with the current energy concept, different effective measures exist for targeted adjustment of the energy balance – and thereby the temperature levels of the soil – and thus over the years of operation, a sustainable and also energy efficient management and use of the geothermal field can be achieved in the long term. Over the three years of operation investigated, despite temporarily increased or decreased temperature levels occurring within the individual years due to the direct influence of heat input and withdrawal, by carrying out manual changes in the operation, it was ultimately possible to return to the original ground temperature level of about 11 °C.

Nevertheless, by use of ultrasonic flow measurement and further temperature profiles of energy piles, an inhomogeneous flow through the geothermal system was found. Because of insufficient performance of the circulating pump, hydraulic adjustment was not possible. Replacement of the corresponding circulating pumps seems to be the only way to fix this issue. The main measure to balance heat input and withdrawal was the expansion – both in terms of time as well as intensity – of the cooling operations so far. However, for the future years of operation a type of portfolio should be created for the targeted adjustment of the energy balance of the ground, which could further contain additional cooling and warming of the soil by using the re-coolers and adjustment of the heat supply with respect to the shares of geothermal energy and local heating. In addition, a solar thermal system for even better performance and increased efficiency could be installed. Automated control of the building operation, taking into account the management of the geothermal field in terms of adjusting temperature levels in the soil, is necessary in future for the sustainability and energy efficiency of the building's energy supply. In this context, a model predictive control would be optimal, and should be investigated.

CRediT authorship contribution statement

Kristian Duus: Conceptualization, Methodology, Validation, Formal analysis, Investigation, Data curation, Writing - original draft, Visualization, Project administration. **Gerhard Schmitz:** Conceptualization, Writing - review & editing, Supervision, Project administration, Funding acquisition.

Declaration of Competing Interest

The authors declare that they have no known competing financial interests or personal relationships that could have appeared to influence the work reported in this paper.

Acknowledgements

This work is being conducted within the framework of a project funded by the Federal Ministry for Economic Affairs and Energy (www.bmwi.de), cf. project funding number 03ET1139A and Sprinkenhof GmbH (www.sprinkenhof.de).

References

[1] Federal Ministry for Economic Affairs and Energy. Draft of the Integrated National Energy and Climate Plan, 2019, URL https://www.bmwi.de/Redaktion/EN/Downloads/E/draft-of-the-integrated-national-energy-and-climate-plan.pdf?__blob=publicationFile&v=5 – Date of access: 09.10.2019.
[2] Senate of the Free and Hanseatic City of Hamburg, Hamburg Climate Plan, 2015, Printed Paper 21/2521. URL https://www.hamburg.de/contentblob/9051304/754a498fcf4e4bbf9516e1f9a99e2bfe/data/d-21-2521-hamburg-climate-plan.pdf – Date of access: 09.10.2019.
[3] K. Duus, G. Schmitz, Energy-optimised Construction: Monitoring of the New Building of the Ministry for Urban Development and Environment in Hamburg, 2018, URL https://www.tib.eu/de/suchen/id/TIBKAT%3A1024844803/IMOBS-Energieoptimiertes-Bauen-Intensivmonitoring/ – Date of access: 09.10.2019.
[4] J. Gao, A. Li, X. Xu, W. Gang, T. Yan, Ground heat exchangers: applications, technology integration and potentials for zero energy buildings, Renewable Energy 128 (2018) 337–349.
[5] G. Florides, S. Kalogirou, Ground heat exchangers – a review of systems, models and applications, Renewable Energy 32 (2007) 2461–2478.
[6] U. Eicker, C. Vorschulze, Potential of geothermal heat exchangers for office building climatisation, Renewable Energy 34 (2009) 1126–1133.
[7] X.Q. Zhai, Y. Yang, Experience on the application of a ground source heat pump system in an archives building, Energy Build. 43 (2011) 3263–3270.
[8] Y. Hwang, J. Lee, Y. Jeong, K. Koo, D. Lee, I. Kim, S. Jin, S. Kim, Cooling performance of a vertical ground-coupled heat pump system installed in a school building, Renewable Energy 34 (2009) 578–582.
[9] A. Michopoulos, T. Zachariadis, N. Kyriakis, Operation characteristics and experience of a ground source heat pump system with a vertical ground heat exchanger, Energy 51 (2013) 349–357.
[10] C. Montagud, J.M. Corberán, Á. Montero, J.F. Urchueguía, Analysis of the energy performance of a ground source heat pump system after five years of operation, Energy Build. 43 (2011) 3618–3626.
[11] X.G. Li, Z.H. Chen, J. Zhao, Simulation and experiment on the thermal performance of U-vertical ground coupled heat exchanger, Appl. Therm. Eng. 26 (2006) 1564–1571.
[12] J. Luo, J. Rohn, M. Bayer, A. Priess, L. Wilkmann, W. Xiang, Heating and cooling performance analysis of a ground source heat pump system in Southern Germany, Geothermics 53 (2015) 57–66.
[13] S.S. Naicker, S.J. Rees, Performance analysis of a large geothermal heating and cooling system, Renewable Energy 122 (2018) 429–442.
[14] H.J.L. Witte, A.J. Van Gelder, H.Ö. Paksoy (Eds.), Three Years Monitoring of a Borehole Thermal Energy Store of a UK Office building. Thermal Energy Storage for Sustainable Energy Consumption, Springer, 2007, pp. 205–219.
[15] S. Li, W. Yang, X. Zhang, Soil temperature distribution around a U-tube heat exchanger in a multi-function ground source heat pump system, Appl. Therm. Eng. 29 (2009) 3679–3686.
[16] B.B. Dehghan, Effectiveness of using spiral ground heat exchangers in ground source heat pump system of a building for district heating/cooling purposes: comparison among different configurations, Appl. Therm. Eng. 130 (2017) 1489–1506.
[17] G. Bode, J. Fütterer, D. Müller, Mode and storage load based control of a complex building system with a geothermal field, Energy Build. 158 (2018) 1337–1345.
[18] VDI 4640, Part 1: Thermal Use of the Underground – Fundamentals, Approvals, Environmental Aspects, Beuth, Berlin, Germany, 2010.
[19] VDI 3807, Part 1: Characteristic Consumption Values for Buildings – Fundamentals, Beuth, Berlin, Germany, 2013.